Subtraction of signal overlaps in Rutherford backscattering spectrometry

Z. L. Liau
Lincoln Laboratory, Massachusetts Institute of Technology, Lexington, Massachusetts 02173

(Received 25 April 1979; accepted for publication 17 September 1979)

A technique has been developed to deduce the individual signals from overlapped ones in Rutherford backscattering spectra. Based on the backscattering kinematics, a coordinate shift and a subtraction are carried out between the backscattering spectra taken at two slightly different incident-ion energies. The subtraction eliminates one of the overlapping signals and yields the derivative of the other one, from which the two individual signals are reconstructed unoverlapped. Before the subtraction, a small change in energy scale is used to correct the slight change of signal shape due to the variation of incident-ion energy. This technique has been tested to yield good results in a computer-simulated backscattering experiment on a thin-film structure consisting of 5 layers of Au-Ag alloys.

PACS numbers: 82.80. − d, 34.40. + n, 29.70.Gn, 68.90. + g

Rutherford backscattering spectrometry (RBS) has been recognized as a nondestructive, qualitative, and fast technique for obtaining compositional and structural information in surface layers of several thousand angstroms.[1] However, there have been substantial restrictions in the use of this powerful technique. For example, one has to use thin-film samples with large mass differences between the constituent elements, otherwise, one often gets overlapped signals which result in uncertainties in data interpretation. In some cases, special sample configurations can be used to avoid the problem.[2] In general, computer simulation can be used (on a trial and error basis) to understand the overlapped signals.[3] Using a different approach, we have developed in this work a new technique in which the individual signals can be obtained from the overlapped ones by a proper subtraction between two RBS spectra of slightly different incident-ion energies.

Figure 1 illustrates the main idea of this technique. In Fig. 1(a), $f_1(E)$ and $g_1(E)$ represent the backscattering signals of two different elements F and G, respectively, in the target which has been analyzed with an incident-ion-energy E_1. Since $f_1(E)$ and $g_1(E)$ overlap, it is the sum of the two signals, $h_1(E) \equiv f_1(E) + g_1(E)$, that is obtained in the RBS experiment. When a slightly higher incident-ion energy E_2 is used for the same experiment, the signals will appear in higher-energy regions as shown in Fig. 1(b). We first assume that the energy dependence of ion-energy loss in the target materials is so small that the individual signals are shifted without changes in shape, i.e.,

$$f_2(E) = f_1(E - K_F \Delta E), \tag{1a}$$

$$g_2(E) = g_1(E - K_G \Delta E), \tag{1b}$$

where K_F and K_G are the backscattering kinematic factors[1] of elements F and G, respectively, and $\Delta E \equiv E_2 - E_1$. (It is also assumed that the energy dependence of the Rutherford cross section has been compensated by a change in integrated ion charge, such that $f_2(E)$ and $f_1(E)$ are of equal amplitudes.) Therefore

$$\begin{aligned} h_2(E) &\equiv f_2(E) + g_2(E) \\ &= f_1(E - K_F \Delta E) + g_1[E - K_F \Delta E \\ &\quad + (K_F - K_G)\Delta E]. \end{aligned} \tag{2}$$

Define

$$\tilde{E} \equiv E + K_F \Delta E. \tag{3}$$

Equation (2) is then transformed into

$$h_2(\tilde{E}) = f_1(E) + g_1(E + \delta E), \tag{4}$$

where

$$\delta E \equiv (K_F - K_G)\Delta E. \tag{5}$$

Because δE is relatively small, Eq. (4) can be written as

$$h_2(\tilde{E}) \cong h_1(E) + \frac{dg_1(E)}{dE}\delta E, \tag{6}$$

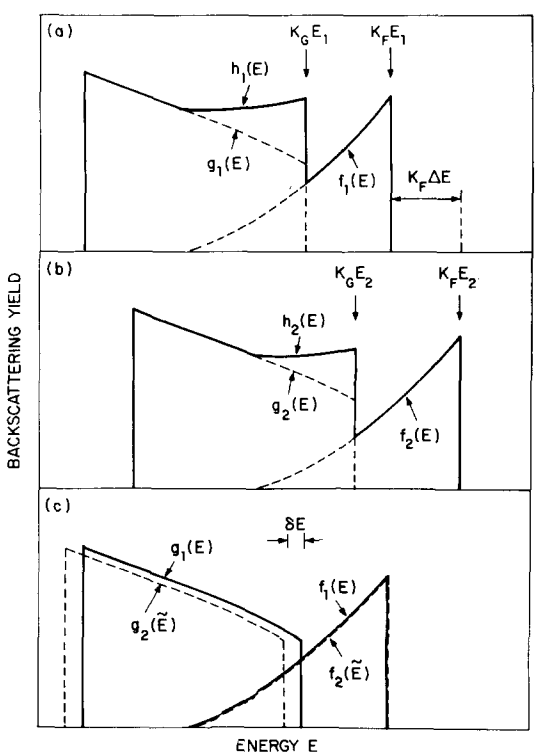

FIG. 1. Illustration of the main idea in the present technique. Parts (a) and (b) represent RBS spectra of a sample taken at incident-ion energies E_1 and E_2, respectively, with $E_2 > E_1$. Part (c) shows the matching of the two spectra in (a) and (b).

 0003-6951/80/010051-03$00.50

which then yields

$$g_1(E) \cong \int \frac{h_2(\tilde{E}) - h_1(E)}{\delta E}\, dE\,. \tag{7}$$

The physical picture of the formulations is illustrated in Fig. 1(c). The function $h_2(\tilde{E})$ actually represents a translation of $h_2(E)$ to a lower-energy region by a distance $K_F \Delta E$, which makes $f_2(\tilde{E})$ coincide completely with $f_1(E)$. But, $g_2(\tilde{E})$ is mismatched with $g_1(E)$ by a small energy distance δE. Therefore, the subtraction between $h_2(\tilde{E})$ and $h_1(E)$ yields the derivative of $g_1(E)$, from which $g_1(E)$ can be reconstructed.

Equations (1a) and (1b) neglect the energy dependence of ion-energy loss in the target material. In energy regions of general interest, the ion-energy loss decreases slowly with ion energy.[1] This results in a slight "shrink" of signals in the lateral direction in the RBS spectrum when a higher incident-ion energy is used. A "shrink rate" s is now introduced:

$$[\epsilon(E_2)] = (1 - s\Delta E)[\epsilon(E_1)]\,, \tag{8}$$

where $[\epsilon(E_1)]$ and $[\epsilon(E_2)]$ are the corresponding stopping cross section factors[1] at incident-ion energies E_1 and E_2, respectively. Based on the $[\epsilon]$ values tabulated by Ziegler and Chu,[4,1] the s value of a thin-film target of a single element is quite constant over a fairly large energy range of interest, as illustrated in Table I. For a compound target, the situation can be more complicated. For simplicity, we assume that s can be approximated as a constant over the whole spectrum and can be obtained experimentally by comparing the "clean" portions of the spectra in the high-energy regions, where there are no signal overlaps. Thus, in addition to a shift by a distance $K_F \Delta E$, the energy scale of $h_2(E)$ should then be expanded by a factor of $(1 + s\Delta E)$ such that $f_2(\tilde{E})$ matches with $f_1(E)$ completely. Because of this expansion, the relative energy shift, δE, between $g_1(E)$ and $g_2(\tilde{E})$ will increase by an amount $(K_F - K_G)E_2 s\Delta E$. Thus the total δE is given by

$$\delta E = (K_F - K_G)\Delta E + (K_F - K_G)E_2 s\Delta E\,. \tag{9}$$

To test this technique, we present a numerical example in which the computer program developed by Ziegler, Lever, and Hirvonen[3] is used to simulate the backscattering experiment. Spectra of 2.0- and 2.1-MeV $^4He^+$ backscattering are obtained for a sample consisting of 5 layers (400 Å each) of Au_xAg_{1-x}, as shown in Fig. 2(a). The $^4He^+$ dose used for the 2.1-MeV spectrum is 1.106 times that of the 2.0-MeV one, such that the clean Au signals in the high-energy regions are of equal heights. The energy scale for the 2.1-MeV spectrum is 3.92 keV per channel as compared to 4.00 keV per channel for the 2.0-MeV one. This corresponds to an s

TABLE I. Shrink rate of spectral width of thin elemental Ag and Au films in $^4He^+$ Backscattering.

	Energy Range (MeV)	
	1.6–1.8	1.8–2.0
Ag	1.97×10^{-4}/keV	2.00×10^{-4}
Au	1.38×10^{-4}	1.37×10^{-4}

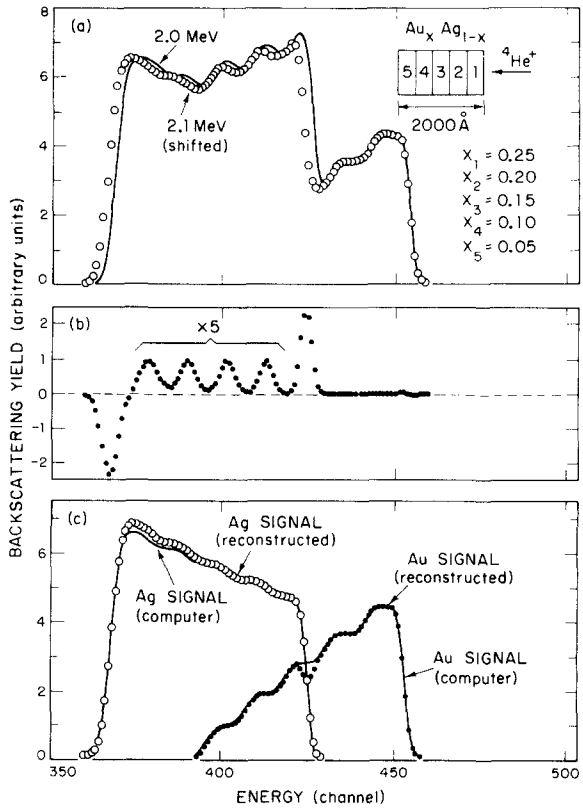

FIG. 2. An example of the present technique. Part (a) shows computer-simulated RBS spectra of the Au_xAg_{1-x} sample. Part (b) shows the difference between the two matched spectra in (a). Part (c) shows the reconstructed as well as the original Ag and Au signals.

value of 2.0×10^{-4}/keV or $s\Delta E = 2.0\times10^{-2}$, which is close to that of Ag in Table I (consistent with the fact that Ag is the dominant species in the sample). The δE as obtained by using Eq. (9) is 8.28 keV. Figure 2(b) shows the difference between the two matched spectra in Fig. 2(a). Starting from the high-energy region, the integration of Eq. (7) is carried out by summing the readings in Fig. 2(b), channel by channel. This integration yields the reconstructed Ag signal shown in Fig. 2(c). The reconstructed Au signal is then obtained as the difference between the 2.0-MeV spectrum in Fig. 2(a) and the reconstructed Ag signal in Fig. 2(c).

The computer generates the individual Ag and Au signals as well as the overlapped ones in Fig. 2(a). Comparisons in Fig. 2(c) show that the present technique has closely reproduced the computer-generated signals in large portions of the spectrum. Larger discrepancies are found in the reconstructed Au signal near the Ag edge. This is probably due to the rapid changes of the Ag signal near the Ag edge which cause larger errors in approximating $g_1(E + \delta E) - g_1(E)$ as $(dg_1/dE)\delta E$ in Eq. (6). There is also a gradual increase in discrepancy between the two Ag signals in the lower-energy region in Fig. 2(c). We suggest that this can be caused by the slightly faster rising rate of the Ag signal of the 2.0-MeV spectrum than that of the 2.1-MeV one, due to the energy dependence of the Rutherford cross section. Although the difference is very small [causing a ~0.5% difference in the two corresponding Ag-signal heights near the low-energy edges of the spectra in Fig. 2(a)], the error can accumulate

because of the integration procedure used in obtaining the reconstructed Ag signal. Calculations show that the error rises nearly parabolically, with a magnitude of a few % near the low-energy edge of the Ag signal, which is comparable to that observed in Fig. 2(c).

Because of its mathematical nature, the present technique can be applied to RBS spectra of samples with lateral nonuniformities. It can also be applied in RBS study of samples containing more than two elements (with signal overlaps between any two of them). One crucial approximation used in this technique is that the shrink of signals can be corrected by a single parameter s. Although this approximation appears to be a good one in the case of Fig. 2, we do not know how good it is in other systems, especially those with extreme compositional nonuniformity. Another major problem will be counting statistics in the real RBS experiments, which can result in large random errors after applying the present technique. In principle, this can be improved by taking as good counting statistics as possible. It may also be desirable to curve fit the RBS spectra in order to eliminate the random errors.

In conclusion, we have demonstrated that individual signals can be obtained to high accuracies from the overlapped ones, by using a simple analytical technique which is mainly based on backscattering kinematics. The general validity of the approximation that the dependence of signal shapes on the incident-ion energy can be compensated by a simple change of energy scale is yet to be evaluated. Should this question be answered, the present technique can become very useful in RBS study of materials with moderate mass differences between the constituent elements.

The author is indebted to E.B. Owens and J.L. Ryan, for the RBS work on Au/InP alloying (which has initiated the present work) and the introduction to the computer simulation. He also wishes to thank A.G. Foyt and C.E. Hurwitz, for their interest and discussions. This work was sponsored by the Department of the Air Force.

[1]See, for example, W.K. Chu, J.W. Mayer, and M.-A. Nicolet, *Backscattering Spectrometry* (Academic, New York, 1978).
[2]R.G. Kirsch, J.M. Poate, and M. Eibschutz, Appl. Phys. Lett. **29**, 772 (1976).
[3]J.F. Ziegler, R.F. Lever, and J.K. Hirvonen, in *Ion Beam Surface Layer Analysis*, edited by O. Meyer, G. Linker and F. Kappeler (Plenum, New York, 1976) Vol. 1, p. 163.
[4]J.F. Ziegler and W.K. Chu, At. Nucl. Data Tables **13**, 463 (1974).

Shallow-homojunction GaAs cells with high resistance to 1-MeV electron radiation

John C. C. Fan, Ralph L. Chapman, and Carl O. Bozler
Lincoln Laboratory, Massachusetts Insitute of Technology, Lexington, Massachusetts 02173

Peter J. Drevinsky
Rome Air Development Center, Deputy for Electronic Technology, Hanscom AFB, Massachusetts 01731

(Received 23 July 1979; accepted for publication 5 October 1979)

We have recently reported the fabrication of single-crystal GaAs shallow-homojunction solar cells that have conversion efficiencies of about 20% at AM1 (17% at AM0). These cells employ an $n^+/p/p^+$ structure, prepared by chemical vapor deposition on either GaAs or Ge substrates. We have now demonstrated the superior resistance of such cells to 1-MeV electron radiation, which produces effects approximating those due to space radiation. The experiments were done on four cells at fluences up to 10^{16} e/cm^2. One of the cells was found to have both higher initial and final maximum power per unit area than any space cells previously reported.

PACS numbers: 84.60.Jt, 78.90. + t, 78.70. − g, 84.60. − h

Although Si solar cells have been extensively used in space, GaAs cells are now emerging as promising candidates for space applications such as space vehicles and solar-power satellites, with a number of potential advantages over Si cells. Since the absorption length for sunlight in GaAs is only about 2 μm, [1] 2 orders of magnitude less than in Si, GaAs cells should exhibit less radiation damage in space, because damage generated more than a few absorption lengths beneath the surface should have little effect on photocurrent collection. In addition, the theoretical conversion efficiency is higher for GaAs than for Si, [2] and GaAs cells operate better than Si cells at elevated temperature [2] and high solar concentrations. [3] Furthermore, the stronger absorption of sunlight in GaAs should allow a significant reduction in cell thickness and therefore weight. In this letter we report the results of initial experiments on the resistance of shallow-homojunction GaAs cells to 1-MeV electron radiation. These results are highly encouraging, suggesting that such cells could be more resistant to the radiation of the space environment than either Si cells or GaAlAs/GaAs hetero-

 0003-6951/80/010053-04$00.50